DOI: 10.13009/EUCASS2017-608

7TH EUROPEAN CONFERENCE FOR AERONAUTICS AND AEROSPACE SCIENCES (EUCASS)

DOI: ADD DOINUMBER HERE

Modeling scalar mixing and transport in LRE-like conditions

Pasquale Eduardo Lapenna†*, Rachele Lamioni and Francesco Creta*

Dept. of Mechanical and Aerospace Engineering,
University of Rome 'La Sapienza', Rome, Italy
pasquale.lapenna@uniroma1.it
†Corresponding author

Abstract

In order to shed light on super- and trans-critical mixing, data from direct numerical simulations of turbulent jets using accurate real gas equation of state as well as thermodynamic and transport properties are analyzed. The influence of super- and trans-critical thermodynamic conditions, typical of liquid rocket engines thrust chambers, on the jet turbulent kinetic energy spectral characteristics are investigated. Moreover modeling issues of thermodynamic and transport properties are investigated and quantitatively evaluated over typical LES/RANS cell sizes.

1. Introduction

Liquid Rocket Engines (LRE) thrust chambers usually operate at high pressures causing mixing and combustion of the propellants to occur under supercritical pressure conditions. Under these severe thermodynamic conditions, the injection temperature of the reactants can be below the pseudo-boiling temperature, hence *transcritical*. As a consequence, abrupt variations of thermodynamic and transport properties are experienced by the mixture during the mixing and combustion processes.[26] In the framework of transcritical non-premixed combustion in LRE-like configurations, the rate of combustion is mainly controlled by turbulent mixing[20] prompting substantial interest in transcritical mixing.

Experimental studies, devoted to the injection and mixing of cryogenic fluids (usually nitrogen) into warm chambers at supercritical pressures, highlighted the strong influence of real gas effects on the jet behavior.[10,15] The cryogenic jets have been recognized very sensitive to the strong density-temperature coupling and to the elevated heat capacity in the proximity of the pseudo-boiling temperature.[4,14] However, several difficulties arises dealing with experiments characterized by such extreme pressure and temperature conditions limiting the fidelity of the quantitative results as well as their physical interpretation.[1] In particular, the detection of small-scale structures and the relevant statistical fluctuation data are still not easily achieved, motivating a substantial research effort in the numerical simulations. Relevant physical insights of the interactions between transcritical thermodynamic conditions and a turbulent flowfield were gleaned from two and three dimensional large eddy simulation (LES) studies by Zong et al.[27,28] However, the interactions between pseudo-boiling and a turbulent flow-field can be consistently addressed only by means of direct numerical simulation (DNS).

In DNS context, transcritical mixing was studied in a temporally evolving mixing layer configuration by Tani et al.,[21] revealing that the turbulent transport mechanisms of momentum and heat can be considered mildly affected by the pseudo-boiling. A slower increase of the temperature inside the jet together with relatively weak fluctuations were found by Terashima and Koshi[24] investigating two-dimensional planar and three-dimensional round nitrogen jets. Transcritical effects were also recently addressed, from the numerical point of view by Terashima et al.[22,23] and Ma et al.[13] They highlighted the necessity of a proper numerical treatment of the sharp density and fluid properties gradients caused by pseudo-boiling, in particular dealing with compressible solvers. A different approach was recently proposed for DNS of transcritical mixing,[11] coupling the lack of acoustic perturbations in the low-mach number limit with high order methods to deal with sub-Kolmogorov scales.

In the present work, drawing from a recently developed DNS database of transcritical and supercritical mixing,[11] peculiar aspect of real fluid flows simulated in the low-Mach number limit are discussed. Firstly the low-Mach number conditions of the DNS database are further assessed. Secondly the different spectral characteristics of turbulent kinetic energy between supercritical and transcritical jets are investigated. Finally modeling issues related to scalar mixing and transport in LRE-like conditions are investigated evaluated over typical LES/RANS cell sizes.

DOI: 10.13009/EUCASS2017-608

2. The DNS database

Classically mixing under severe thermodynamic conditions, such as those encountered in LRE combustion chambers, have been investigated numerically by means of fully compressible solvers. The latter invariably use conservative formulations that have been shown to produce serious numerical problems from the numerical scheme stability point of view. Due to strong nonlinearities of the thermodynamic system, in particular in the pseudo boiling region, spurious pressure oscillations can cause serious stability issues. Moreover the problem cannot be mitigated by introducing numerical dissipation from using lower-order schemes or artificial viscosity, as pointed out in a recent work by Ma et al.[13]

In this context, a different approach has been proposed in a recent work[11] in which a low Mach number approximation has been used to overcome the issues mentioned above. In the low-Mach number limit, the governing equations of a flow are recast by filtering out the acoustic wave propagation. Therefore the thermodynamic or background pressure p_0 is considered constant allowing an efficient numerical integration of the equations while density variations caused by thermal non-homogeneity are still fully taken into account.[25]

Table 1: Physical and numerical parameters summary.

	Case 3	Case 4
Difference in velocity streams ΔU_{jet} (m/s)	0.09	0.116
Initial jet width H (mm)	1	1
Reference kinematic viscosity ν_{ref} (m/s^2)	$5.92 \cdot 10^{-8}$	$7.74 \cdot 10^{-8}$
Initial jet Reynolds number $Re_{jet} = \Delta U_{jet} H/\nu_{ref}$	1500	1500
Jet time unit $t_{jet} = H/\Delta U$ (ms)	11.3	8.6
Jet Mach number $M_{jet} = \Delta U/a_{jet}$	$3.4 \cdot 10^{-4}$	$5.7 \cdot 10^{-4}$
Environment Mach number $M_{env} = \Delta U/a_{env}$	$2.5 \cdot 10^{-4}$	$3.2 \cdot 10^{-4}$
Density ratio ρ_{jet}/ρ_{env}	10.14	3.63
Domain size L_xxL_yxL_z (mm)	6x6x3	6x6x3
Grid points	$\approx$ 144 Million	$\approx$ 43 Million
Initial velocity perturbations u_{rms}	$0.05\Delta U$	$0.05\Delta U$
Initial velocity perturbations integral scale l_0	$H/3$	$H/3$
Kolmogorov scale η_K (mm)	0.0297	0.0297
Batchelor scale η_B (mm)	0.0106	0.0228

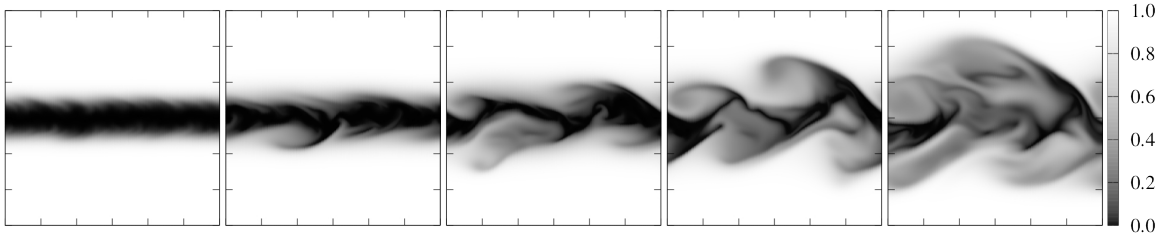

(a)

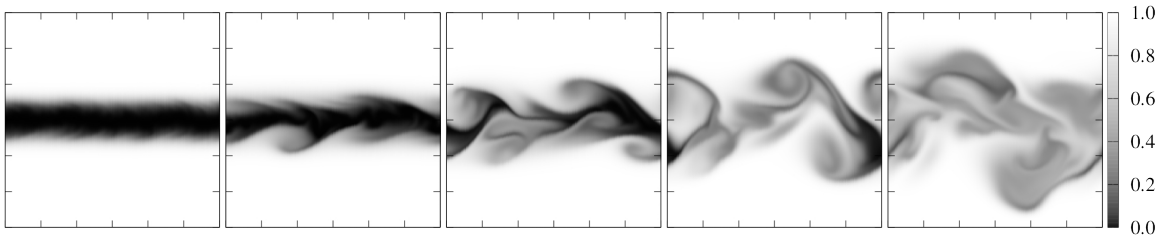

(b)

Figure 1: Evolution of the ξ field for the transcritical (a) and supercritical (b) temporal jet at five representative time instants $t^* = t/t_{jet} = 1, 5, 10, 15, 20$.

DOI: 10.13009/EUCASS2017-608

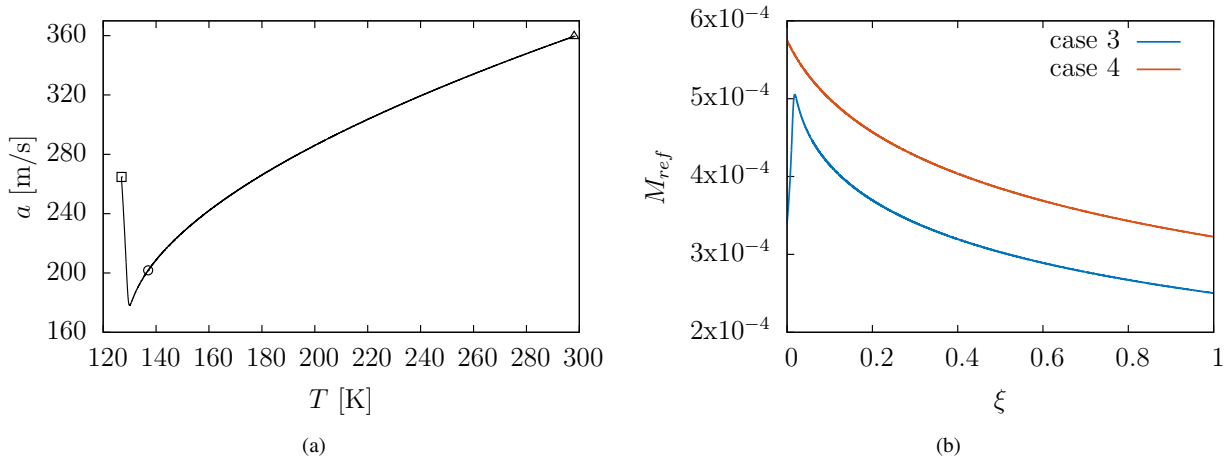

(a) (b)

Figure 2: Panel (a): speed of sound at $p_0 = 39.7$ bar as a function of the temperature, symbols indicate (△) the environment conditions and the initial jet conditions for (□) case 3 and (◯) case 4. Panel (b): Reference Mach number at $p_0 = 39.7$ bar as a function of the non dimensional temperature for the two cases considered.

The DNS database that is used in the present work[11] has been created using a modified version of the massively parallel, incompressible and low-Mach number spectral element method (SEM)[5,16]-based CFD code `nek5000`[6] coupled with constant pressure tabulated real fluid properties for nitrogen by means of the National Institute for Standards and Technology (NIST) `Refprop` software.[12] The SEM-based high-order discretization allows to correctly resolve the large thermodynamic variations caused by the pseudo-boiling, with a reasonable number of grid points. The thermodynamic conditions of the planar temporal jet configuration used, were chosen to match the experiments of cryogenic injection of nitrogen at supercritical pressures, performed by Mayer et al.[4,14] Two cases from the original experimental test matrix were considered: a transcritical case and a supercritical case corresponding respectively to cases 3 and 4 in the experiments.[14] Simulation characteristics are summarized in Tab. 1 while spanwise cuts of the dimensionless temperature field $\xi = T - T_{jet}/T_{env} - T_{jet}$ are shown in fig.1

In order to further asses the low-Mach conditions for the transcritical and supercritical mixing cases, a reference Mach number can be defined: $M_{ref} = \Delta U/a$ based on the velocity difference between the jet and the environment and on the speed of sound at $p_0 = 39.7$ bar as shown in Fig. 2 which experiences a drop across the pseudocritical temperature. Note that local velocities greater than ΔU are not experienced in any of the two simulations (case 3 and case 4) as clearly observable in Fig. 3; for this reason we can consider the definition of M_{ref} amply conservative.

The hydrodynamic (or perturbation) pressure p_1 can be denoted as $p_1(x,t) = p(x,t) - p_0(t)$, where $p(x,t)$ is the pressure field and $p_0(t)$ the uniform background pressure, which is constant in the open domain considered. Such hydrodynamic pressure is an $O(M^2)$ deviation from the background pressure so that $p_1/p_0 = O(M^2)$. Fig. 3 displays the pdfs of the computed p_1, showing the extremely limited range of hydrodynamic pressures as expected from the low Mach numbers at play. Indeed, a reference pressure disturbance can be estimated as $\delta p \approx p_0 \max(M_{ref}^2)$, based on the maximum reference Mach number. We obtain for the transcritical case $\delta p \approx 1.03 \cdot 10^{-5}$ bar while for the supercritical case $\delta p \approx 1.29 \cdot 10^{-5}$ bar. These pressure perturbations are largely insufficient to influence the constant pressure property tabulation in any significant way.

3. Results and discussion

The temporal evolution of the transcritical and supercritical jet shown in Fig. 1 highlights some fundamental differences. The transcritical jet qualitatively resembles a liquid-like jet break-up during its time evolution, in spite of the vanishing surface tension which confines the fluid to a single supercritical phase. This liquid-like behavior, which is absent in the supercritical jet, is induced by the pseudo-boiling process between the core of the jet, which is characterized by liquid-like densities, and the warm environment which has gas-like properties. Contrary to the commonly encountered subcritical vaporization, the pseudo-boiling is a continuous, highly stratified processes having a diffuse interface without a distinct phase change. While this allows a single phase approach, it needs to be taken into account in sub-grid scale modeling of mixing and transport, as it occurs on characteristics length scale well below LES/RANS grid sizes.

DOI: 10.13009/EUCASS2017-608

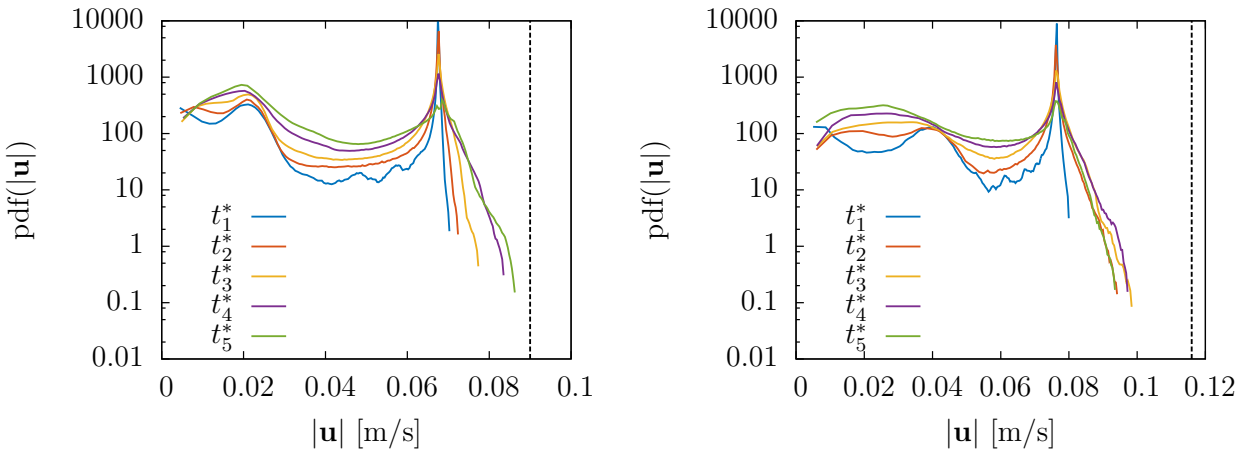

(a) Case 3 (b) Case 4

Figure 3: Probability density functions of the velocity magnitude for the transcritical jet (case 3) and the supercritical jet (case 4) at five representative time instants $t^* = 1, 5, 10, 15, 20$. Vertical dashed line corresponds to $|\mathbf{u}| = \Delta U$.

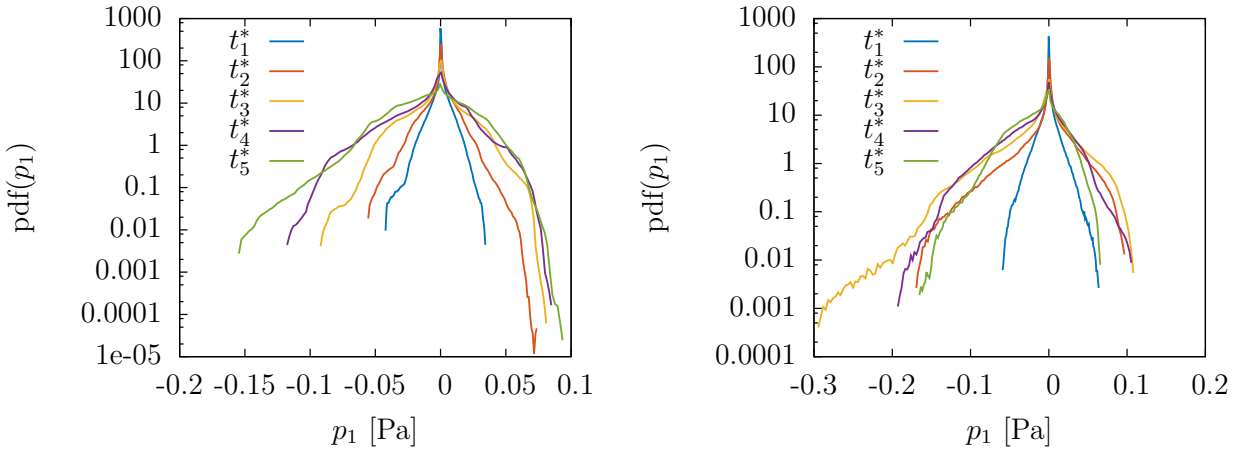

(a) Case 3 (b) Case 4

Figure 4: Probability density functions of the hydrodynamic pressure for the transcritical jet (case 3) and the supercritical jet (case 4) at five representative time instants $t^* = 1, 5, 10, 15, 20$.

DOI: 10.13009/EUCASS2017-608

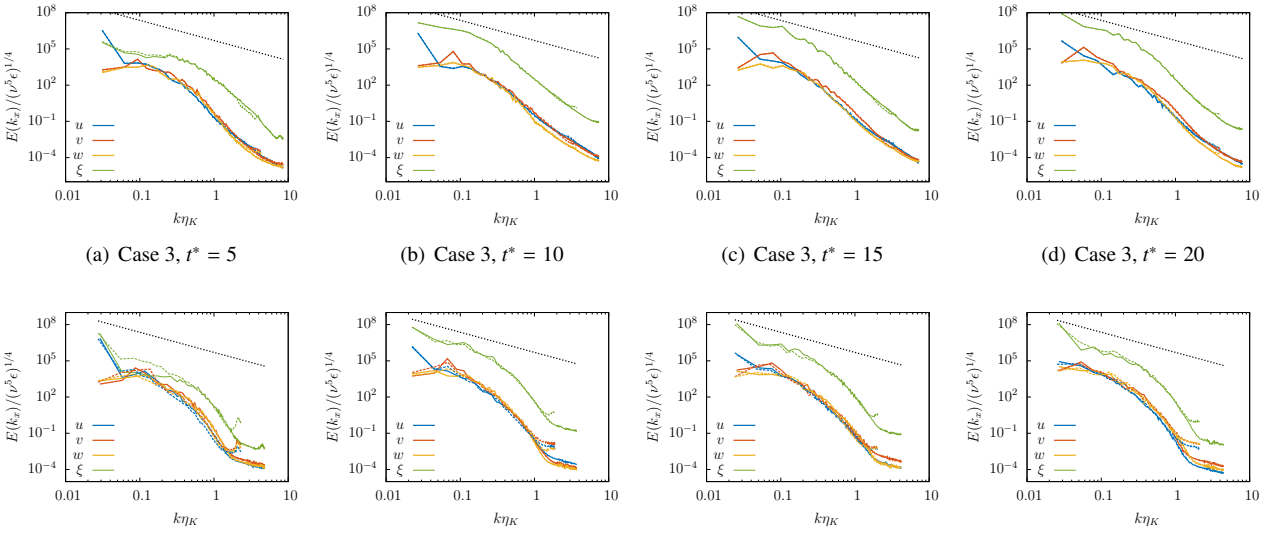

(a) Case 3, $t^* = 5$ (b) Case 3, $t^* = 10$ (c) Case 3, $t^* = 15$ (d) Case 3, $t^* = 20$

(e) Case 4, $t^* = 5$ (f) Case 4, $t^* = 10$ (g) Case 4, $t^* = 15$ (h) Case 4, $t^* = 20$

Figure 5: Streamwise, one dimensional spectral densities of the u, v, w and ξ for the transcritical jet (case 3) and the supercritical jet (case 4) at four representative time instants $t^* = 5$, 10, 15, 20. The spectra are scaled in Kolmogorov units η_K and the dashed lines represent the $-5/3$ slope. Colored dashed lines are the results obtained with the coarse grids, characterized by the half of the spectral resolution.

3.1 Spectral characteristics in supercritical and transcritical conditions

In order to investigate the spectral characteristics and structural differences between transcritical and supercritical jets the one-dimensional energy spectra for the velocity components (u, v and w) and for the non dimensional temperature (ξ) have been computed in both streamwise and spanwise directions in the jet centerline for 4 representative time instants ($t^* = 5$, 10, 15, 20). The spectra are consistently scaled using Kolmogorov units $k\eta_K$.[19]

Figure 5 and 6 shows respectively the streamwise and spanwise spectral densities of the velocity components and the dimensionless temperature. Both the transcritical and supercritical jets show good resolution characteristics by having no energy accumulation at the smallest scales, confirming that the smallest fluid scales expected are completely resolved. In addition also the results from coarse grid simulations are shown in order to confirm the DNS-type resolution of the data. Indeed the coarse grids can be observed to faithfully reproduce the spectral content of the nominal grids. The effects of the relatively low initial jet Reynolds number are clearly observable due to the limited extension of the inertial range.

In both the transcritical and supercritical case the ξ spectrum extend well over $k\eta_K = 1$ confirming that, in the near critical conditions considered, residual scalar stratifications at sub-Kolmogorov scales are present. This results from the elevated fluid Prandtl number, defined as $Pr = \lambda/\rho C_p \nu_{ref}$, which spans a wide range of values over unity. Under $Pr > 1$ conditions, a length scale smaller than the turbulence smallest scale, i.e. the Kolmogorov scale η_K, is in principle to be expected.[2] This scale is usually referred to as the Batchelor scale η_B, where $\eta_B \sim \eta_K Pr^{-1/2}$[3] and represents the smallest length scale in scalar concentration. As a result the temperature spectra, with respect to $k\eta_K$ extends more in the transcritical case rather than in the supercritical case since the former is characterized by a relatively high Prandtl number ($Pr \approx 7.85$) while the latter being relatively close to unity ($Pr \approx 1.65$). However a substantial research effort is needed in order to asses the influence of pseudo boiling on dissipation scales.

3.2 Subgrid scale modeling of thermodynamic and transport properties

In order to include turbulence-chemistry interaction in turbulent combustion modeling of non-premixed flames, one of the most used technique is the presumed pdf approach. The use of presumed pdf approaches for turbulent combustion modeling in LES/RANS framework allow a simple expression by means of a convolution operator with a pdf, of every filtered thermochemistry related variable, such as thermodynamic and transport properties. Therefore these quantities can be expressed as:[18]

DOI: 10.13009/EUCASS2017-608

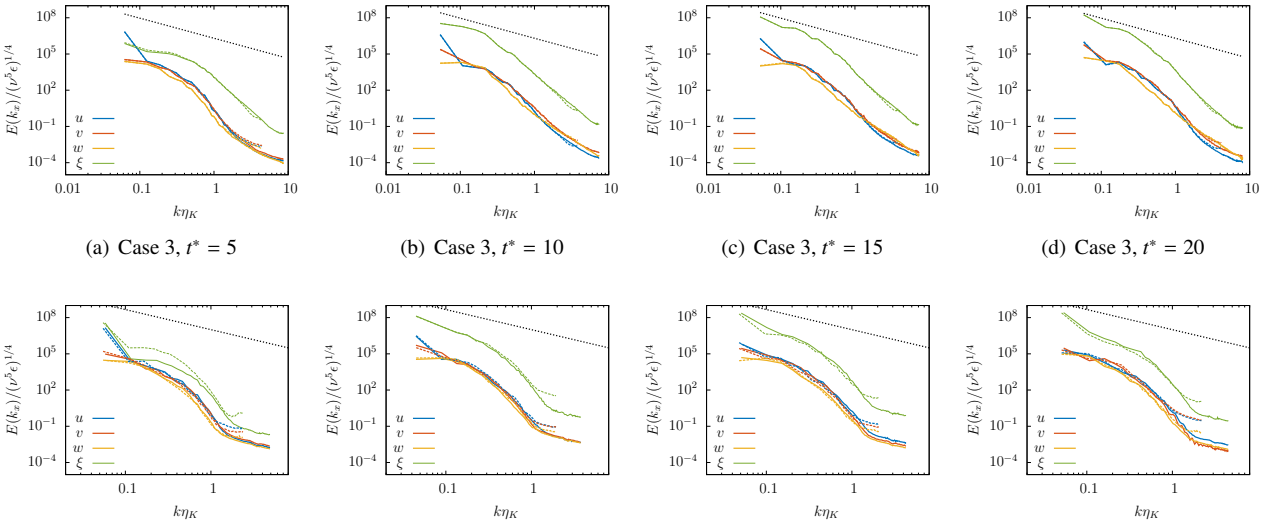

(a) Case 3, $t^* = 5$ (b) Case 3, $t^* = 10$ (c) Case 3, $t^* = 15$ (d) Case 3, $t^* = 20$

(e) Case 4, $t^* = 5$ (f) Case 4, $t^* = 10$ (g) Case 4, $t^* = 15$ (h) Case 4, $t^* = 20$

Figure 6: Spanwise, one dimensional spectral densities of the u, v, w and ξ for the transcritical jet (case 3) and the supercritical jet (case 4) at four representative time instants $t^* = 5$, 10, 15, 20. The spectra are scaled in Kolmogorov units η_K and the dashed lines represent the $-5/3$ slope. Colored dashed lines are the results obtained with the coarse grids, characterized by the half of the spectral resolution.

$$\overline{\Psi} = \int_0^{\chi_{max}} \int_0^1 \Psi(\xi^*, \chi^*) p(\xi^*) p(\chi^*) d\xi^* d\chi^* \tag{1}$$

where ξ is the mixture fraction [1], χ is the scalar dissipation rate of ξ, $p(\xi^*)$ and $p(\chi^*)$ are respectively the sub-grid presumed pdf of ξ and χ which are considered statistically independent.

The statistics of these two quantities govern the turbulence-chemistry interactions and therefore the modeling of scalar mixing. Presumed shapes of the pdfs have generally been developed under ideal gas assumptions[18] motivating the present investigation in the effects of the transcritical conditions on scalar mixing and dissipation rate. Therefore *a priori* testing, using DNS data, of the widespread presumed pdf methods are carried out under consistent transcritical thermodynamic conditions.

In the present analysis, attention will be devoted only to scalar mixing statistics, hence to $p(\xi^*)$, since the majority LES approach neglect the sub-grid variance of χ. The latter assumptions is commonly used since the large part of the turbulent motion is resolved on the computational grid.[17]

A commonly employed presumed shape of $p(\xi^*)$, in the context of passive scalar mixing for TCM, is the β-pdf,[7–9] which needs a reduced set of statistical information, consisting of only two parameters, to be completely determined. The parameters needed by the β-pdf, denoted here by Γ, are the mean of the mixing variable $\overline{\xi}$ and its variance $\overline{\xi'\xi'}$:

$$p(\xi^*) \approx \Gamma(\xi^*; \overline{\xi}, \overline{\xi'\xi'}). \tag{2}$$

In *a-priori* tests, the input data for the sub-grid models is taken directly from the filtered DNS simulations. Three different levels of approximation will be considered for the pdf $p(\xi^*)$ of Eq.(1):

- **Exact or DNS**: in which the pdf $p(\xi^*)$ is extracted by directly filtering the DNS data.
- **β-model**: in which the pdf $p(\xi^*)$ is assumed to be a β-function distribution $\Gamma(\xi^*; \overline{\xi}, \overline{\xi'\xi'})$ based on mean and variance of ξ extracted from DNS data.
- **No-model**: in which the pdf $p(\xi^*)$ is assumed to be a Dirac delta $\delta(\xi^* - \overline{\xi})$ centered at the mean value of ξ extracted from the DNS data.

[1] Since the DNS database is limited to a non-reactive case the so called mixture fraction will be associated to the non dimensional temperature ξ.

DOI: 10.13009/EUCASS2017-608

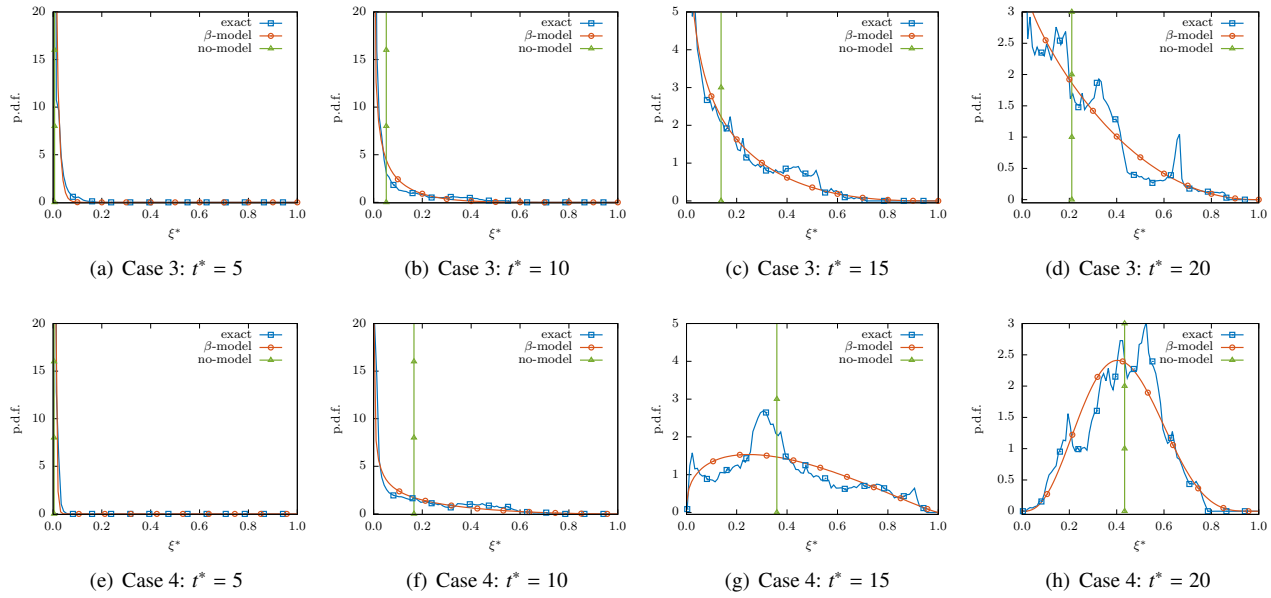

(a) Case 3: $t^* = 5$ (b) Case 3: $t^* = 10$ (c) Case 3: $t^* = 15$ (d) Case 3: $t^* = 20$

(e) Case 4: $t^* = 5$ (f) Case 4: $t^* = 10$ (g) Case 4: $t^* = 15$ (h) Case 4: $t^* = 20$

Figure 7: Pdf of the non-dimensional temperature for the transcritical (left column) and supercritical (right column) jet, at four representative time instants.

Figure 7 the exact pdf's of the non-dimensional temperature ξ are compared with the β-function type distribution based on the DNS-data and with the no-model approximation. The results show a good agreement between the β-model and the exact distribution over the four representative time instants considered, and for both the transcritical and supercritical cases. This suggests that the β-pdf is an accurate model of the exact distribution provided that the first two moments are correctly captured. On the other hand the no-model exhibits obvious limitations especially when the pdf profiles become wider due to turbulent mixing. Indeed, the no-model approach possess no additional information about the sub-grid fluctuations of the stochastic variable, other than its mean $\overline{\xi}$. This limitation directly impacts on point-wise evaluation of the thermodynamic and transport properties in a LES/RANS framework, since this depends on the local scalar field of ξ inside the computational cell.

The performance of the above mentioned models can be assessed using the DNS results averaged on the jet centerline, to define a global error as:

$$\varepsilon^*(\Delta_{filt}) = \int_0^{t_{final}} \frac{|\overline{\Psi}_{DNS} - \overline{\Psi}_{mod}|}{\overline{\Psi}_{DNS}} dt^* \tag{3}$$

where $\overline{\Psi}$ is a generic thermodynamic or transport properties evaluated by means of DNS or by a model (β-model or no-model) as denoted by the subscripts. The error ε^* measures the discrepancies between the DNS results and the two models presented, and it clearly depends on Δ_{filt} which represent the LES/RANS grid size chosen.

Figure 8 displays the error defined by eq. 3 for both the transcritical and supercritical case using the β-model and the no-model, as functions of the ratio between the LES/RANS a priori filter grid size and the original DNS grid size. The global error of both approaches, as expected tends to zero as Δ_{filt} approaches Δ_{DNS} and the SGS scalar variance progressively reduces as an increasing part of the turbulent fluctuations gets captured by a finer grid. Focusing our attention only on coarse grids $\Delta_{filt}/\Delta_{DNS} > 10$ which are of practical interest, it is clearly observable that accounting for the sub-grid scalar variance of ξ with a presumed pdf substantially improves the results. This implies that given an appropriate resolution and a turbulence closure model, using a sub-grid model for the scalar variance of the non-dimensional temperature allows the use of a coarser LES/RANS grid for $Pr > 1$ supercritical and transcritical flows such as those encountered in LRE combustion chambers. Particularly relevant are the errors, using the no-model, in the density evaluation of the transcritical case as shown in fig. 8(a). On the other hand transport properties are shown to be less sensitive to the test grid size used. The overall relative magnitude of the errors suggest that neglecting the sub-grid variance for a supercritical flow leads to large but relatively confined errors. On the contrary in the presence of pseudo boiling modeling the the sub-grid scalar variance can be crucial in particular using relatively coarse grids.

DOI: 10.13009/EUCASS2017-608

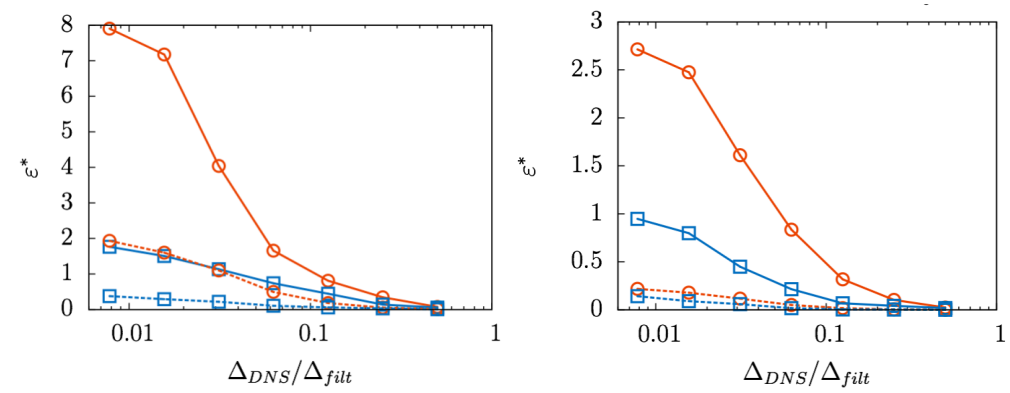

(a) density

(b) constant pressure heat capacity

(c) thermal conductivity

(d) dynamic viscosity

Figure 8: Modeling errors of both thermodynamic and transport properties as function of the ratio between LES/RANS grid size Δ_{filt} and DNS resolution Δ_{DNS}

DOI: 10.13009/EUCASS2017-608

4. Conclusions

Data from a recently developed database DNS of transcritical and supercritical turbulent jets using accurate real gas equation of state as well as thermodynamic and transport properties have been analyzed.

The spectral densities of the velocity components and the dimensionless temperature have been calculated taking advantage of the homogeneous directions of the temporal evolving jet configuration. The spectra at various non-dimensional jet time have evidenced that the temperature spectra, with respect to $k\eta_K$ extends more in the transcritical case rather than in the supercritical case since the former is characterized by a relatively high Prandtl number ($Pr \approx 7.85$) while the latter being relatively close to unity ($Pr \approx 1.65$).

Mixing related modeling issues of thermodynamic and transport properties have been investigated in the context of presumed pdf approaches and quantitatively evaluated over typical LES/RANS cell sizes. Results have evidenced that pseudo-boiling, typical of transcritical flows, is inherently a sub-grid scale phenomenon that needs to be taken into account in LES/RANS modeling. The use a presumed β-pdf for the sub-grid temperature statistical distribution has shown to significantly improve the thermodynamic and transport properties evaluation.

5. Acknowledgments

Participants of this study were financially supported by the Italian Ministry of University and Research (MIUR). The authors acknowledge the Italian Super-Computing Interuniversity Consortium CINECA for support and high-performance computing resources under Grant No. DL-DNS/HP10CRXOHF.

References

[1] Daniel T Banuti and Klaus Hannemann. The absence of a dense potential core in supercritical injection: A thermal break-up mechanism. *Physics of Fluids (1994-present)*, 28(3):035103, 2016.

[2] GK Batchelor. Small-scale variation of convected quantities like temperature in turbulent fluid part 1. general discussion and the case of small conductivity. *Journal of Fluid Mechanics*, 5(01):113–133, 1959.

[3] GK Batchelor, ID Howells, and AA Townsend. Small-scale variation of convected quantities like temperature in turbulent fluid part 2. the case of large conductivity. *Journal of Fluid Mechanics*, 5(01):134–139, 1959.

[4] Richard Branam and Wolfgang Mayer. Characterization of cryogenic injection at supercritical pressure. *J. Propul. Power*, 19:342–355, 2003.

[5] Michel O Deville, Paul F Fischer, and Ernest H Mund. High-order methods for incompressible fluid flow. 9, 2002.

[6] Paul F Fischer, James W Lottes, and Stefan G Kerkemeier. nek5000 web page. *http://nek5000.mcs.anl.gov*, 2008.

[7] Sharath S Girimaji. Modeling turbulent scalar mixing as enhanced diffusion. *Combustion science and technology*, 97(1-3):85–98, 1994.

[8] Sharath S Girimaji and Ye Zhou. Analysis and modeling of subgrid scalar mixing using numerical data. *Physics of Fluids (1994-present)*, 8(5):1224–1236, 1996.

[9] SS Girimaji. Assumed β-pdf model for turbulent mixing: Validation and extension to multiple scalar mixing. *Combustion Science and Technology*, 78(4-6):177–196, 1991.

[10] Wolfgang O H. Mayer, Axel H A. Schik, Bruno Vielle, Christian Chauveau, Iskender G-ograve, kalp, Douglas G Talley, and Rodger D Woodward. Atomization and breakup of cryogenic propellants under high-pressure subcritical and supercritical conditions. *Journal of Propulsion and Power*, 14(5):835–842, 1998.

[11] Pasquale Eduardo Lapenna and Francesco Creta. Mixing under transcritical conditions: an a-priori study using direct numerical simulation. *The Journal of Supercritical Fluids*, in press, 2017.

[12] EW Lemmon, ML Huber, and MO McLinden. Refprop: Reference fluid thermodynamic and transport properties. *NIST standard reference database*, 23(8.0), 2007.

[13] Peter C Ma, Yu Lv, and Matthias Ihme. An entropy-stable hybrid scheme for simulations of transcritical real-fluid flows. *Journal of Computational Physics*, 340:330–357, 2017.

DOI: 10.13009/EUCASS2017-608

[14] W Mayer, J Telaar, R Branam, G Schneider, and J Hussong. Raman measurements of cryogenic injection at supercritical pressure. *Heat and Mass Transfer*, 39(8-9):709–719, 2003.

[15] M Oschwald and A Schik. Supercritical nitrogen free jet investigated by spontaneous raman scattering. *Experiments in Fluids*, 27(6):497–506, 1999.

[16] Anthony T Patera. A spectral element method for fluid dynamics: laminar flow in a channel expansion. *Journal of computational Physics*, 54(3):468–488, 1984.

[17] Heinz Pitsch. Large-eddy simulation of turbulent combustion. *Annu. Rev. Fluid Mech.*, 38:453–482, 2006.

[18] Thierry Poinsot and Denis Veynante. *Theoretical and numerical combustion*. RT Edwards Inc., Philadelphia, PA, 2005.

[19] Stephen B Pope. *Turbulent flows*. Cambridge University Press, UK, 2000.

[20] G. Singla, P. Scouflaire, C. Rolon, and S. Candel. Transcritical oxygen/transcritical or supercritical methane combustion. *Proc. Combust. Inst.*, 30:2921–2928, 2005.

[21] Hiroumi Tani, Susumu Teramoto, Nobuhiro Yamanishi, and Koji Okamoto. A numerical study on a temporal mixing layer under transcritical conditions. *Computers & Fluids*, 85:93–104, 2013.

[22] Hiroshi Terashima and Mitsuo Koshi. Approach for simulating gas–liquid-like flows under supercritical pressures using a high-order central differencing scheme. *Journal of Computational Physics*, 231(20):6907–6923, 2012.

[23] Hiroshi Terashima and Mitsuo Koshi. Strategy for simulating supercritical cryogenic jets using high-order schemes. *Computers & Fluids*, 85:39–46, 2013.

[24] Hiroshi Terashima and Mitsuo Koshi. Unique characteristics of cryogenic nitrogen jets under supercritical pressures. *Journal of Propulsion and Power*, 29(6):1328–1336, 2013.

[25] AG Tomboulides, JCY Lee, and SA Orszag. Numerical simulation of low mach number reactive flows. *Journal of Scientific Computing*, 12(2):139–167, 1997.

[26] Vigor Yang. Modeling of supercritical vaporization, mixing, and combustion processes in liquid-fueled propulsion systems. *Proc. Combust. Inst.*, 28:925–942, 2000.

[27] Nan Zong, Hua Meng, Shih-Yang Hsieh, and Vigor Yang. A numerical study of cryogenic fluid injection and mixing under supercritical conditions. *Physics of Fluids (1994-present)*, 16(12):4248–4261, 2004.

[28] Nan Zong and Vigor Yang. Cryogenic fluid jets and mixing layers in transcritical and supercritical environments. *Combustion Science and Technology*, 178(1-3):193–227, 2006.